PEER REVIEW, Vol. 5, Nº 17, 2023
DOI: 10.53660/692.prw2209
ISSN: 1541-1389

Evaluation of different models of tumor spheroid generation with CAL27 cells

Avaliação de diferentes modelos de geração de esferoides tumorais com células CAL27

Leilane de Sousa Mendonça
ORCID: https://orcid.org/0000-0001-7827-6056
Federal University of Amazonas, Brazil
E-mail: leilane.smendonca@gmail.com
Laura Luiza Moreira da Silva Dias
ORCID: https://orcid.org/0009-0001-0207-8288
Federal University of Amazonas, Brazil
E-mail: lauraluizamsd98@gmail.com
Hector Henrique Ferreira Koolen
ORCID: https://orcid.org/0000-0002-0181-348X
Universidade Federal do Amazonas, Brasil
E-mail: hectorkoolen@gmail.com
Emersom Silva Lima
ORCID: https://orcid.org/0000-0002-9367-2812
Federal University of Amazonas, Brazil
E-mail: eslima@ufam.edu.br
Marne Carvalho de Vasconcellos
ORCID: https://orcid.org/0000-0001-7785-4029
Federal University of Amazonas, Brazil
E-mail: marne@ufam.edu.br

ABSTRACT

In cancer research, three-dimensional cell culture models have become useful tools for investigating the tumor microenvironment, cancer stages, and the search for new therapeutic targets. In this sense, the aim of this study was to contribute with a tumor spheroid model of squamous cell carcinoma (CAL27) to be used for studies of this type of cancer and new therapeutic alternatives. For this, two methods of spheroid generation were tested, a 96-well plate model coated with agarose and a cylindrical microwell model developed using 9x9 size micromolds with 800 µm diameter that fit into 24-well plates (3D Petri Dish®). The microwell generation model showed more promising results, generating spheroids up to 183.97 ± 15 µm in diameter. Although the analysis of spheroid size and growth kinetics was superior to other assays, the marking of the necrotic center produced essential images for confirmation of the generation of the three-dimensional model, as well as the results of the cytotoxicity assay. The results presented here contribute to the progress of the use of 3D cell culture systems for the study and search for responses to agents that may act on squamous cell carcinoma and provide a viable alternative for cancer research laboratories.

Keywords: 3D culture; Skin cancer; Alternative methods; Tumor cell; cancer.

Recebido: 20/06/2023 | Aceito: 23/07/2023 | Publicado: 26/07/2023

RESUMO

Na investigação do câncer, os modelos de cultura celular tridimensional têm se tornado modelos para investigar o microambiente tumoral, estágios do câncer e na pesquisa de novos alvos terapêuticos. Nesse sentido, o objetivo desse estudo foi contribuir com um modelo de esferoide tumoral de carcinoma de células escamosas (CAL27), a fim de ser utilizado para estudos desse tipo de câncer e de novas alternativas terapêuticas. Para isso foram testados dois métodos de geração de esferoides, modelo em placa de 96 poços recobertos com agarose e com micropoços desenvolvidos usando micromoldes no tamanho 9x9 com 800 µm de diametero que se encaixam em placas de 24 poços (3D Petri Dish®). O modelo de geração com micromoldes apresentou resultados mais promissores, com geração de esferoides de até 183,97±15 µm de diâmetro. Embora a análise do tamanho e cinética de crescimento dos esferoides fosse superior a outros ensaios, a marcação do centro necrótico produziu imagens essenciais para confirmação da geração do modelo tridimensional, bem como os resultados do ensaio de citotoxicidade. Os resultados aqui apresentados, contribuem com o progresso do emprego de sistemas de cultura celular 3D para estudo na busca de resposta para testes de agentes que possam atuar em carcinoma de células escamosas e fornecer uma alternativa viável para os laboratórios de pesquisa que estudam o câncer.

Palavras-chave: Cultura 3D; Câncer de pele; Métodos alternativos; Célula tumoral; câncer.

INTRODUCTION

Non-melanoma skin cancer is considered the most frequent type of cancer in the world population, being one of the most invasive and aggressive cancers (FERLAY et al., 2019; WHO, 2020). In 2020, estimates from the Global Cancer Observatory (Globocan), indicate that there were 19.3 million new cancer cases and 18.1 million non-melanoma skin cancer cases (FERLAY et al., 2019; SUNG et al., 2021). In Brazil, estimates indicate 101,920 cases of non-melanoma skin cancer in men and 118,570 cases in women in 2023, with the southern, central-western, and southeastern regions having the highest incidence in men, followed by the northeastern and northern regions. For women, non-melanoma skin cancer is more incident in all Brazilian regions (BRASIL, 2022).

Squamous Cell Carcinoma (SCC) is the second most common type of skin cancer, after basal cell carcinoma, and can affect various parts of the body, including the skin, lips, mouth, esophagus, trachea, bronchi, bladder, and genitals. There is no precise estimate of the incidence of this type of cancer in Brazil, as incidence data is only collected in some regions of the country and can vary widely depending on factors such as age, sex, geographic region, and exposure to risk factors such as smoking and excessive exposure to sunlight, infection by some types of viruses, such as the Human Papillomavirus (CHAMOLI et al., 2021; QUE; ZWALD; SCHMULTS, 2018).

The symptoms of SCC can include non-healing sores, scaly or crusty patches on the skin or mucous membranes, lumps or nodules, and changes in the color or texture of the skin. Treatment of SCC depends on the stage of the disease and the location of the tumor, and may include surgery, radiation therapy, chemotherapy, or biological therapies. The prognosis of SCC varies depending on various factors such as the stage of the disease, age, and overall health of the patient, but early detection and appropriate treatment increase the chances of a cure (SHIMIZU et al., 2011).

Squamous cell carcinoma arises from changes in keratinocytes, the cells that make up the epithelial tissue, and understanding how these alterations affect the biological functions of the skin, as well as evaluating the presence and intensity of these changes in response to external substances, is essential for the development of effective cancer treatments and for understanding the environment in which the tumor develops (MAAS-SZABOWSKI; STÄRKER; FUSENIG, 2003; REIJNDERS et al., 2015).

The tumor microenvironment is characterized by interactions between tumor cells and the different components of the surrounding tissue, such as immune cells, stromal cells, and blood vessels, to promote tumor growth and dissemination. It also contains bioactive substances, including hormones, extracellular matrix, chemokines, cytokines, growth factors, and enzymes, whose dynamic action coordinates intercellular communication. Changes in the tumor microenvironment can affect the response to cancer treatment, and understanding the role of the tumor microenvironment is critical for the development of new cancer therapies and improving clinical outcomes for patients (MBEUNKUI; JOHANN, 2009).

Studies have sought to simulate the tumor microenvironment in vitro, particularly using three-dimensional (3D) culture, as they are more representative in relation to molecular mechanisms, tumor architecture, and cellular heterogeneity, facilitating the development and screening of new anti-tumor therapies. Studies indicate that 3D models are capable of more accurately representing the interactions between cancer cells and the microenvironment, as well as allowing for a more precise assessment of tumor response to treatments. These models are useful in identifying new therapies and diagnostic and prognostic biomarkers, as well as in the development of personalized cancer therapies. Therefore, 3D models are promising tools to improve our understanding of cancer and to accelerate the development of new treatments (ASTASHKINA; MANN; GRAINGER, 2012; COSTARD et al., 2021).

One of the widely used three-dimensional models for studying cancer is the spheroid culture, where a small aggregate of cells grows free from foreign materials, as a new method of manufacturing microenvironments that allows the creation of a large number of complex and highly reproducible tissues, which can be used for evaluating substances with anti-tumor action, as well as for analyzing tumor biology and cellular behavior in this environment (FENNEMA et al., 2013; GUNTI et al., 2021; MEHTA et al., 2012).

In oncology research, several studies have shown that tumors grown in monolayer are sensitive to various chemotherapeutic agents, while the same cells grown in spheroid form are resistant to them. On the other hand, some drugs are only effective in a 3D environment. In addition, 3D spheroid models are ideal for evaluating the long-term effects of drugs, as tumor cells can remain functionally stable for several weeks, better

representing the architecture and microenvironment of the tumor (VERJANS et al., 2018).

The use of tumor spheroid models can increase the predictive power of in vitro drug screening tests, offering a more ethical and aligned alternative to animal experimentation methods in obtaining more reliable results. In this context, the present study aims to contribute with a tumor spheroid culture model of squamous cell carcinoma that allows for the investigation of new targets for cancer treatment, in order to enable a more realistic analysis of the tumor microenvironment.

METHODS

Cells and reagents

Squamous cell carcinoma of the tongue (CAL27) were kindly provided by Vanessa Morais Freitas (School of Pharmaceutical Sciences, University of São Paulo). Cell line were grown in 25 cm² culture flasks in Dulbecco's Modified Eagle Medium (DMEM, Life Technologies, Foster City, CA, USA) with 10% fetal bovine serum (FBS, Gibco), with 100 µg/mL streptomycin and 100 U/mL penicillin, and incubated at 37 °C with a 5% CO2 atmosphere. Subculturing was performed using 0,25% Trypsin-EDTA (Gibco) for 5 minutes.

Spheroid preparation

Tumor spheroid were generated from CAL27 cells using the liquid overlay method as previously described (FRIEDRICH et al., 2009; SPOERRI; GUNASINGH; HAASS, 2021). Spheroids were generated in 96-well cell culture flat-bottomed plates previously covered with 1.5% agarose (50 µL total/well) with different seeding densities (500, 1000, 1500, 2000, 3000 total cells/well) to promote formation of a single spheroid per well. Every 3–4 days for incubation, 50% of the medium in each well was replaced with fresh medium (200 µL total/well). Cells were incubated at 37°C with 5% CO2 for 10 days and monitored every 24 hours for analysis of spheroid formation.

Another model tested for generating spheroids with CAL27 was non-adherent agarose gel self-assembly, with cylindrical microwells developed using 9x9 size micromolds with 800 µm diameter that fit into 24-well plates (3D Petri Dish®, MicroTissues Inc., St. Louis, MO, USA). A volume of 500 µL of autoclaved 2% agarose was pipetted into the mold. After 6-8 minutes for polymerization, the agarose was

removed from the mold and placed in one well of the 24-well plate. To balance the 3D Petri Dish®, 1 mL of culture medium was added per well. Two concentrations of CAL27 cells were tested for spheroid formation, 50x104 and 100x104. The cells were placed inside the agarose (180 µL). Spheroid formation was achieved by incubating the plate at 37°C with 5% CO2 injection and monitored every 24 h for up to 7 days using the Carl ZEISS Axio Vert.A1 imaging system with 4× and 10x objective.

Image analysis

Images of all spheroids were taken on day 1, day 3 and day 7 or 10 using Carl ZEISS Axio Vert.A1 optical microscope with the 4× objective to spheroids were generated in 96-well cell culture flat-bottomed plates previously covered with 1.5% agarose and 1, 3 and 7 days for the micromold model. The scale of images was determined using a calibration slide. After incubation image each well of the 96-well plate with a phase-contrast microscope using a 4x objective to monitor and analyze spheroid integrity, diameter and volume. Spheroid analysis was performed through image processing algorithms implemented in the AxioVision 4.5 Software (Zeiss), which allows reliable and reproducible area selection to determine spheroid diameter and volume. The following morphometric information was spheroid area, mean spheroid diameter, spheroid volume, minimum and maximum diameter (FRIEDRICH et al., 2009).

Growth kinetics

Spheroids were generated in 96-well cell culture flat-bottomed plates previously covered with 1.5% agarose (50 µL total/well) with seeding density 3000 cells/well and spheroids were generated using micromold model (MicroTissues® 3D Petri Dish®) with seeding densities 50x104 and 100x104 cells. After 10 and 7 days of incubation at 37°C, 5% CO2 of the spheroids for both models tested, respectively. Spheroid diameter increase was calculated by dividing the difference in spheroid diameter between days by the diameter on day 1 (IVANOV et al., 2014).

$$Dincrease\% = (D\ final\ day - D\ day1)*100/Dday1$$

Alamar blue assay

For the detection of cell viability based on the reduction of resazurin (oxidized form) to resofurin (reduced form), a solution of Alamar Blue (resazurin 7-Hydroxy- 3H-phenoxazin-3-one 10-oxide) 60 µM was prepared in DMEM medium (IVANOV et al., 2014). 150 µL that Alamar Blue solution was distributed to each well and the plate was incubated. Fluorescence was measured using microplate reader DTX 800 Beckman

Coulter Multimode Detector in 465 nm excitation and 540 nm emission 4 h after dye addition.

In the search for promising molecules for cancer treatment, a potentially effective substance was used to test the cell viability of spheroids under in vitro treatment, 22β-hydroxytingenone (22 HTG). 22β-hydroxytingenone (22-HTG) is a triterpenoid of the quinonemethide class that was extracted from *Salacia impressifolia* (Miers) A. C. Smith (Celastraceae family), a plant traditionally used in medicine. This substance has shown promising results in cancer studies in our research laboratory, exhibiting cytotoxic activity against squamous cell carcinoma and melanoma (ARANHA et al., 2021). The extraction workflow for obtaining 22-HTG has been previously described in a study conducted by (ARANHA et al., 2020; DA SILVA et al., 2016). Cisplatin was used as a control substance, as it is commonly used in cancer treatment, including head and neck cancer.

Fluorescent evidence of central necrosis

Fluorescent staining ethidium bromide (EB)/acridine orange (AO) (Sigma-Aldrich) was performed to evidence of central necrosis. The spheroids washed with PBS, after which, were stained with 5 μg/mL of acridine orange/ethidium bromide (AO/EB) solution, and the images captured using a Nikon Ti Eclipse microscope at 4× magnification. The difference between dye permeability into intact cell membrane makes it possible to identify viable, apoptotic, and necrotic cells. Green cells are stained only with AO and represent viable cells, green and orange cells represent apoptotic cells and are stained with both AO and EB, finally necrotic cells are orang and stained with EB.

Statistical analysis

All data were presented as the mean ± standard deviation (SD) from three independent experiments performed in triplicate. Statistic difference ($p<0.05$) was obtained by analysis of variance (ANOVA) followed by Tukey's posttest using GraphPad Prism 6.0 for Windows (Institute Software for Science, San Diego, CA).

RESULTS AND DISCUSSION

Formation of CAL27 spheroids

In order to evaluate the cell behavior for spheroid formation, two generation models were tested: the model with a 96-well plate coated with agarose and the

micromold model (MicroTissues® 3D Petri Dish®). Figure 1 shows the microtissues generated in the 96-well plate, where spheroid formation was observed only at a concentration of 3000 cells per well after 10 days of incubation. The spheroids generated by this model showed a volume retraction every day of incubation, reaching an average diameter of 124.3 µm on the tenth day, at the initial concentration of 3000 cells per well. At the other cell concentrations tested, there was no spheroid formation and when the plate was agitated, they broke apart and the cells returned to being dispersed in the well.

Figure 1. Monitoring of spheroid growth generated in the 96-well plate model coated with agarose. A - Different cell concentrations tested per well; B - Daily monitoring of spheroid formation initiated with 3000 cells per well; C - Images of spheroids with diameter identification after 10 days of culture initiated with 3000 cells per well. Images captured using a Primovert Carl Zeiss microscope. Scale 50 µm.

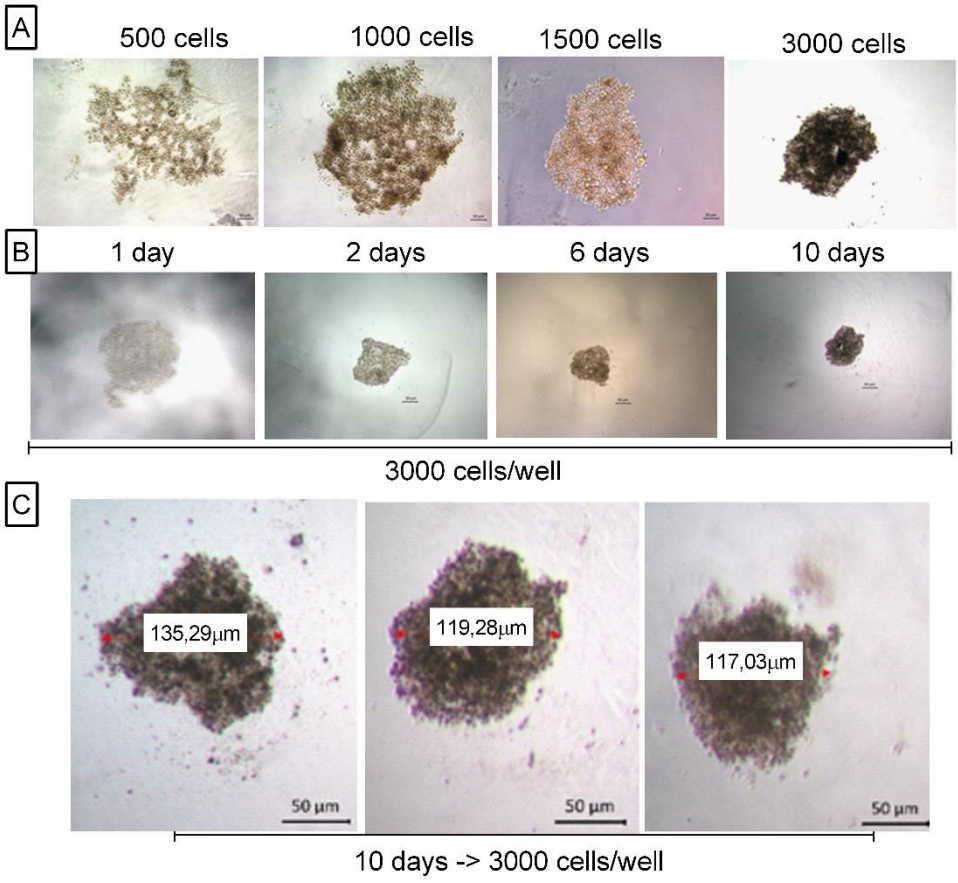

Source: The authors.

To generate spheroids in the 96-well plate model, different CAL27 cell concentrations (500, 1000, 1500, and 3000 cells per well) were tested. However, it was found that the cells did not form stable spherical structures, and with culture medium

renewals, cell disaggregation was observed, even under the best condition identified with 3000 cells per well, which made it impossible to conduct more detailed studies with the spheroids generated by this model. Spheroids generated with the micromold model presented more homogeneous and standardized sizes compared to the 96-well plate model, as shown in Figure 2. From the second day of culture, a more stable and uniform cell aggregate can already be observed in the two CAL27 cell concentrations tested, $50x10^4$ and $100x10^4$ cells added per micromold.

Figure 2. Growth monitoring of 3D spherical microtissues using MicroTissues® 3D Petri Dish® micro-mold spheroids. Brightfield images were acquired with Primovert Carl Zeiss Imaging Systems using a 4x objective.

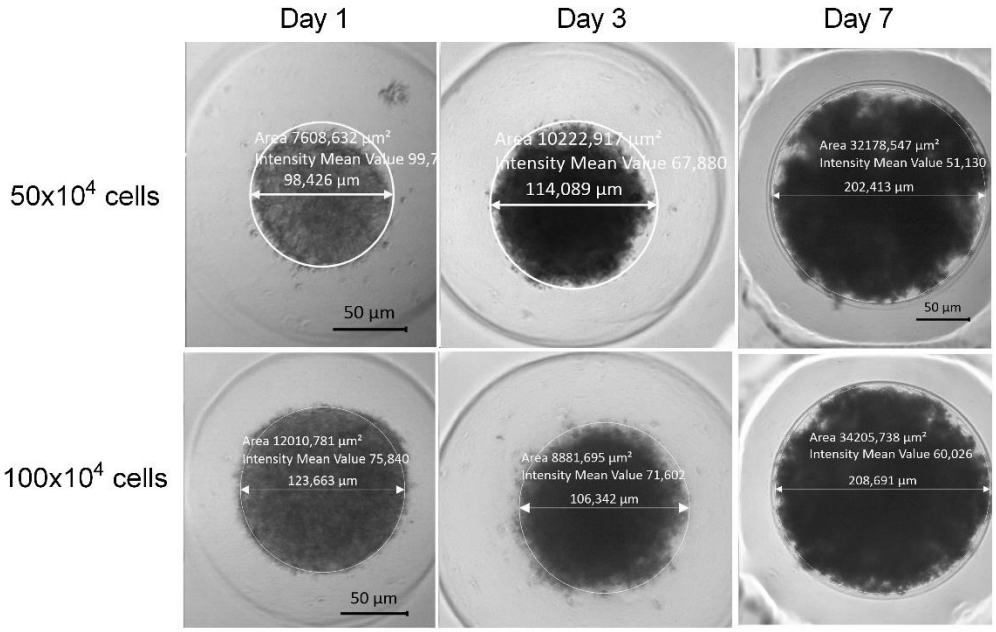

Source: The authors.

We chose to test the micromold model with CAL27 considering the need to optimize the formation of spheroids in terms of quality and quantity, so that it could be easily reproducible and implemented in other laboratories. This technique is simple, offers easy control over the well size, and is compatible with existing techniques, as the cells are spatially confined and the microwells act as centers for cell aggregation. Studies demonstrate that spheroids generated in microwells are more homogeneous in size compared to those generated by conventional techniques (LEE; KIM, 2021).

Analysis of spheroid diameter

One of the first studies that used the 3D co-culture model showed that, over time, the diameter of spheroids from tumor cell lines tends to increase compared to non-tumor cell lines (RAMA-ESENDAGLI et al., 2014). At one day of age, CAL27 spheroids generated by the MicroTissues® 3D Petri Dish® model had a diameter of 91.88±4 µm at the initial density of 50x104 cells compared to 131.07±4 µm at the initial density of 100x104 cells, with a statistically significant difference. The same effect was observed after 7 days of culture, with a diameter of 100.61±10 µm for the density of $50x10^4$ cells and 183.97±15 µm for the density of $100x10^4$ cells (Figure 3).

Figure 3: Monitoring of spheroid growth by diameter and fluorescence intensity analysis using the Alamar Blue method. A - Diameter of spheroids generated with the MicroTissues® 3D Petri Dish® model; B - Fluorescence intensity of spheroids generated with the agarose plate and 3D Petri Dish® MicroTissues model. Results are expressed as mean ± standard deviation of three independent experiments. P-value: (**) p<0.01 (***) p<0.001 and (****) p<0.0001.

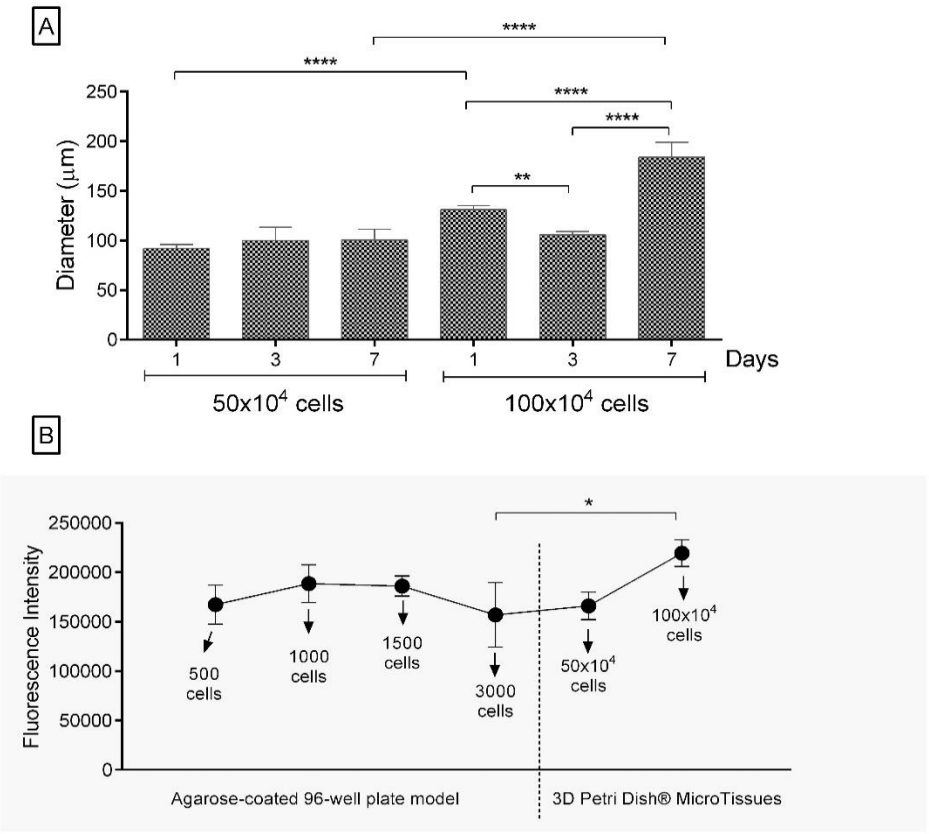

Kinetics of spheroid growth

Spheroid growth, similar to solid tumors, is characterized by an initial phase of volume increase followed by a "spheroidization/stabilization time" where spheroids

become more regular in shape and decrease in volume until they reach a kind of equilibrium. This phase is essential for the structural complexity and functional organization of the spheroid (ZANONI et al., 2019).

Very low cell densities in the initial spheroid generation process resulted in smaller spheroids after the growth period. The highest cell densities tested in both models produced larger spheroids. Spheroid growth using the 3D Petri Dish® generation model showed a 9.4% growth calculated by dividing the difference in spheroid diameter between days by the diameter on day 1 at a concentration of $50x10^4$ cells, compared to 40.36% at a concentration of $100x10^4$ cells after 7 days of culture.

Cell density can have a significant influence on in vitro spheroid formation. Generally, a high enough cell density is required to allow for cellular aggregation and spheroid formation. However, if the cell density is too high, central necrosis may occur within the spheroid due to a lack of oxygen and nutrients for the innermost cells. Additionally, cell density can influence spheroid growth rate and gene expression of the cells comprising the spheroid (ISHIGURO et al., 2017). Therefore, it is important to optimize cell density for each cell type and experimental setup to obtain the best results in in vitro spheroid studies.

Spheroids ability to reduce resazurin

As spheroid structures are often irregular, diameter is not a precise measure for assessing density. Therefore, fluorescence intensity can also serve to evaluate cell density. In addition, to elucidate the viability of using the model as a platform for assays to evaluate cell viability for the discovery of new therapeutic molecules, the reduction of resazurin (oxidized form) to resofurin (reduced form) method - Alamar Blue was chosen. After application of the Alamar Blue solution, fluorescence intensity was analyzed and there was no significant difference between the results using the spheroid generation model in a 96-well plate coated with agarose. In the MicroTissues® 3D Petri Dish® model, there was a trend of increasing fluorescence intensity with increasing initial cell density. Fluorescence intensity was higher in the initial cell density of 100x104 compared to 3000 cells in the model generated in a 96-well plate with agarose (Figure 3).

The cytotoxic activity of antitumor substances was evidenced in the spheroid model. After 48 hours of treatment with 22HTG and cisplatin, there was a reduction in cell viability compared to the negative control of death. Treatment with 22HTG promoted

a 38% reduction in cell viability at a concentration of 1 µM and a 28% reduction at a concentration of 2.5 µM. Cisplatin, tested at a concentration of 10 µM, reduced cell viability by approximately 37% (Figure 4).

In studies conducted by our research group, 22HTG reduced CAL27 viability by 50% in a monolayer model after 48 hours of treatment, at a concentration of 3.014 µM, 95% confidence interval equal to 2.8 to 3.3 µM (PARENTE et al., 2023). When compared to the results achieved in the spheroid model, our study reinforces that tumor spheroids are more resistant to treatment than monolayer models. The same effect was observed with cisplatin, which showed lower cytotoxic potential in the spheroid model compared to monolayer models. Monolayer studies using CAL27 indicate IC50 values (50% inhibitory concentration) below 10 µM after 48 hours of cisplatin treatment (STENZEL et al., 2017; ZHANG et al., 2020).

Figure 4. Percentage of CAL27 cell viability after 48-hour treatment with 22-HTG and cisplatin (10µM). P-value: (****) p<0.0001.

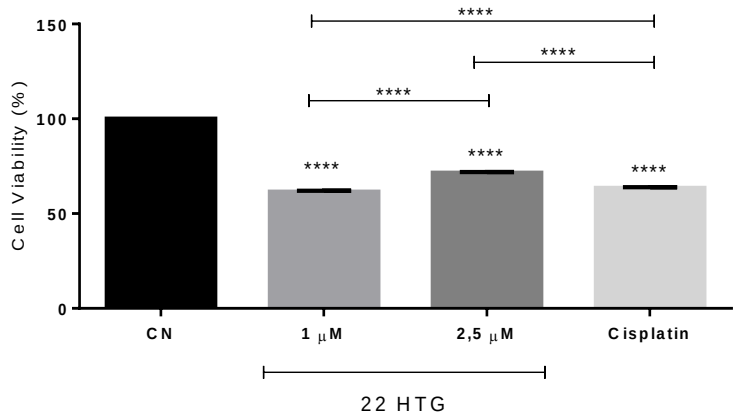

Studies indicate that in vitro tumor spheroids are more resistant to substances compared to monolayer cell culture models due to their three-dimensional architecture and the presence of nutrient and oxygen gradients in their core. Cells in the center of the spheroid have less access to nutrients and oxygen, making them more resistant to chemotherapy treatments that depend on uniform drug distribution in all cells (DÄSTER et al., 2017; ZANONI et al., 2019, 2020). Additionally, the presence of cells in different stages of the cell cycle and cell-cell interactions can also contribute to spheroid resistance to treatment (KOROKNAI et al., 2020; NUNES et al., 2019).

Fluorescent evidence of central necrosis

A spheroid can be divided into three zones, namely, the necrotic zone in the interior, the quiescent zone in the middle, and the proliferative zone on the exterior. Dead cells (quiescent and necrotic zones) may result from lack of nutrition and oxygen in the interior, while external cell proliferation occurs on the surface of the spheroid (HUANG; YU; TANG, 2020; NATH; DEVI, 2016). Acridine Orange and Ethidium Bromide staining were used to visualize the necrotic nucleus and viable cells of the spheroids.

In Figure 4, it is possible to observe the labeling of viable cells in green with Acridine Orange and the necrotic nucleus in red with Ethidium Bromide, evidencing the formation of a hypoxic center in both tested initial cell densities, $50x10^4$ and $100x10^4$ in the MicroTissues® 3D Petri Dish® model. The central cells of the spheroids lose viability due to difficulty in accessing nutrients and oxygen. Due to the three-dimensional nature of spheroids, gradients of nutrients, oxygen, and pH are established over time, resembling the physiological microenvironment of solid tumors in which the distance from blood vessels gives rise to them (BRÜNINGK; RIVENS, 2020).

Figure 5. Representative fluorescence microscopy images of spheroids gerados com o modelo MicroTissues® 3D Petri Dish® nas densidades iniciais de células $50x10^4$ e $100x10^4$ after 7 days. Green fluorescence indicates Acridine orange stain in the live cells and red fluorescence indicates the Ethidium bromide stain in the dead cells. Images were acquired with Imaging Software NIS-Elements 4.30.01 (Nikon Instruments, Melville, NY). Scale bars represent 100 µm.

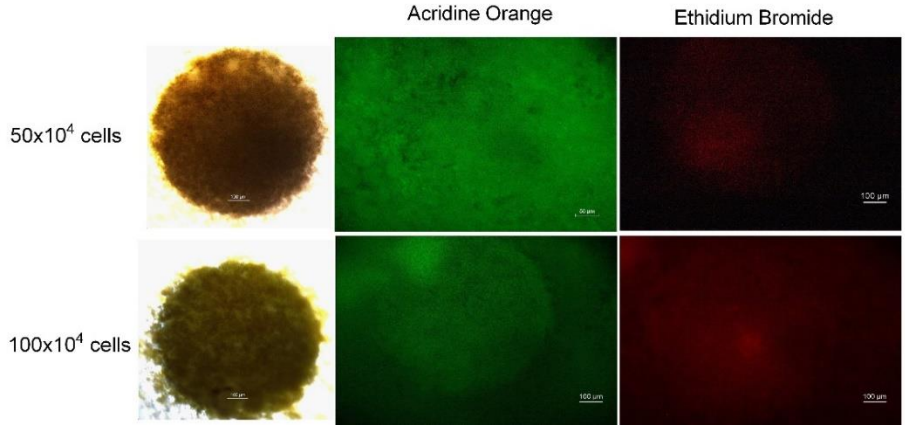

Source: The authors.

In experimental oncology research, studies have shown that tumors grown in a monolayer are sensitive to chemotherapeutic agents, while the same cells grown in spheroid form are resistant to them. On the other hand, some drugs are only effective in a 3D environment. The spheroid model is particularly advantageous for cancer research due to its similarity to non-vascularized tumor nodules, presenting central hypoxia and

different regions of growth. However, it is important to note that spheroids can develop central necrosis, which requires attention from researchers when conducting experiments (SAKALEM et al., 2021; VERJANS et al., 2018).

As spheroids grow in size, the cells in the core have less access to nutrients and oxygen, leading to an initial condition of hypoxia followed by necrosis. While the population of cells in the spheroid core decreases, the opposite is true for the periphery, where a layer of densely packed cells is formed (IVANOV et al., 2014; SONG; NAJJAR; DILLER, 2014). This phenomenon may explain the relatively constant relationship between spheroid size and cell number in this experiment. However, further confirmation of this relationship is necessary.

Figure 6: Representative images of fluorescence microscopy of spheroids generated with the MicroTissues® 3D model treated with 22-βhydroxytingenone (22HTG) at concentrations of 1.25 and 2.5 µM, and Cisplatin at a concentration of 10 µM after 48 hours of treatment. The scale bars represent 100 µm.

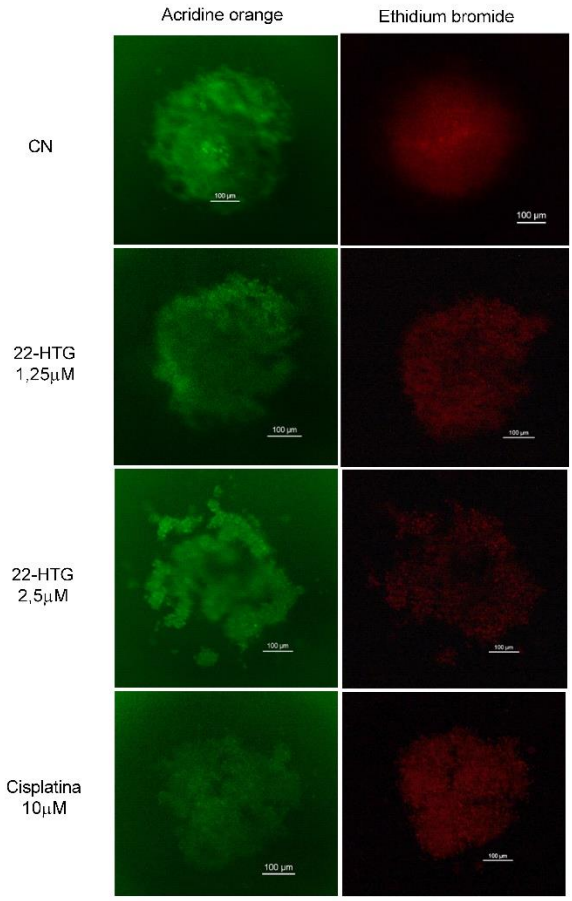

Source: The authors.

The 48-hour treatment with 22-βhydroxytingenone promoted a decrease in the necrotic center and an increase in necrosis in cells at the periphery of the tumor at the tested concentrations of 1.25 and 2.5 µM. The same effect was observed with Cisplatin at a concentration of 10 µM. The effect on cell disaggregation in the spheroids was observed when treated at a concentration of 2.5 µM, thus reinforcing the effect of 22-βhydroxytingenone on CAL27 cell line, even in a three-dimensional spheroid structure (Figure 6).

Studies indicate that the effect of substances on the necrotic center of in vitro-generated tumor spheroids may vary depending on the substance and experimental conditions. The necrotic center forms in tumor spheroids due to a lack of adequate nutrients and oxygen in their interior. This same mechanism occurs in tumors in vivo; however, angiogenesis pathways are activated to promote oxygen supply and survival of tumor cells (DÄSTER et al., 2017; SONG; NAJJAR; DILLER, 2014).

In the SKMEL-28 human melanoma cell line, 22-beta-hydroxytingenone has been shown to reduce cell proliferation, migration, and invasion in a monolayer model (ARANHA et al., 2020, 2021). In a three-dimensional cell culture model, as well as in the CAL27 cell line, 22-βhydroxytingenone had not been previously studied, making the results obtained in this study important contributions. However, it is important to note that the response of tumor cells and the effect of substances in general may vary depending on the tumor type, cell line used, administered doses, and experimental conditions. Therefore, specific studies are needed to evaluate the effect of 22-βhydroxytingenone on the necrotic center of in vitro-generated tumor spheroids.

CONCLUSION

With the results obtained, this research contributes with a tumor spheroid generation model with CAL27 as an alternative to monoculture cell models in order to obtain more reliable results in cancer research, including the search for new therapeutic targets and drugs. However, it is worth noting that these are characterization and standardization assays for spheroid formation and that application assays with standard substances should be carried out to properly determine the use of the model.

ACKNOWLEDGMENTS

The Fundação de Amparo à Pesquisa do Estado do Amazonas (Fapeam) for the fellowship financial support through the POSGRAD UFAM project.

REFERENCES

ARANHA, E. S. P. et al. 22β-hydroxytingenone reduces proliferation and invasion of human melanoma cells. **Toxicology in Vitro**, v. 66, 1 ago. 2020. https://linkinghub.elsevier.com/retrieve/pii/S0887233319307015

ARANHA, E. S. P. et al. 22β-hydroxytingenone induces apoptosis and suppresses invasiveness of melanoma cells by inhibiting MMP-9 activity and MAPK signaling. **Journal of Ethnopharmacology**, v. 267, 1 mar. 2021. https://linkinghub.elsevier.com/retrieve/pii/S0378874120334930

ASTASHKINA, A.; MANN, B.; GRAINGER, D. W. A critical evaluation of in vitro cell culture models for high-throughput drug screening and toxicity. **Pharmacology & Therapeutics**, v. 134, n. 1, p. 82–106, abr. 2012. https://linkinghub.elsevier.com/retrieve/pii/S0163725812000022

BRASIL. **Estimativa 2023: incidência de câncer no Brasil**. Available at: <https://www.inca.gov.br/publicacoes/livros/estimativa-2023-incidencia-de-cancer-no-brasil>. Accessed on: 10 jun. 2023.

BRÜNINGK, S. C.; RIVENS, I. 3D tumour spheroids for the prediction of the effects of radiation and hyperthermia treatments. **Scientific Reports**, v. 10, n. 1653, 2020. https://doi.org/10.1038/s41598-020-58569-4

CHAMOLI, A. et al. Overview of oral cavity squamous cell carcinoma: Risk factors, mechanisms, and diagnostics. **Oral Oncology**, v. 121, 1 out. 2021. https://linkinghub.elsevier.com/retrieve/pii/S136883752100556X

COSTARD, L. S. et al. Influences of the 3D microenvironment on cancer cell behaviour and treatment responsiveness: A recent update on lung, breast and prostate cancer models. **Acta Biomaterialia**, 15 set. 2021. https://linkinghub.elsevier.com/retrieve/pii/S1742706121000507

DA SILVA, F. M. A. et al. Chemical constituents from Salacia impressifolia (Miers) A. C. Smith collected at the Amazon rainforest. **Biochemical Systematics and Ecology**, v. 68, p. 77–80, 1 out. 2016. https://linkinghub.elsevier.com/retrieve/pii/S030519781630165X

DÄSTER, S. et al. Induction of hypoxia and necrosis in multicellular tumor spheroids is associated with resistance to chemotherapy treatment**. Oncotarget**. Available at: <https://doi.org/10.18632/oncotarget>. Accessed on: 14 abr. 2023.

FENNEMA, E. et al. Spheroid culture as a tool for creating 3D complex tissues. **Trends in Biotechnology**, v. 31, n. 2, p. 108–115, fev. 2013. https://linkinghub.elsevier.com/retrieve/pii/S0167779912002223

FERLAY, J. et al. Estimating the global cancer incidence and mortality in 2018: GLOBOCAN sources and methods. **International Journal of Cancer**, v. 144, n. 8, p. 1941–1953, 2019. https://onlinelibrary.wiley.com/doi/10.1002/ijc.31937

FRIEDRICH, J. et al. Spheroid-based drug screen: Considerations and practical approach. **Nature Protocols**, v. 4, n. 3, p. 309–324, 2009. https://www.nature.com/articles/nprot.2008.226

GUNTI, S. et al. Organoid and Spheroid Tumor Models: Techniques and Applications. **Cancers**, v. 13, n. 4, p. 874, 19 fev. 2021. https://www.mdpi.com/2072-6694/13/4/874

HUANG, Z.; YU, P.; TANG, J. Characterization of Triple-Negative Breast Cancer MDA-MB-231 Cell Spheroid Model. **OncoTargets and therapy**, v. 13, p. 5395, 2020. https://www.dovepress.com/characterization-of-triple-negative-breast-cancer-mda-mb-231-cell-sphe-peer-reviewed-article-OTT

ISHIGURO, T. et al. Tumor-derived spheroids: Relevance to cancer stem cells and clinical applications. **Cancer Science**, v. 108, n. 3, p. 283–289, 1 mar. 2017. https://onlinelibrary.wiley.com/doi/10.1111/cas.13155

IVANOV, D. P. et al. Multiplexing spheroid volume, resazurin and acid phosphatase viability assays for high-throughput screening of tumour spheroids and stem cell neurospheres. **PLoS ONE**, v. 9, n. 8, 13 ago. 2014. https://dx.plos.org/10.1371/journal.pone.0103817

KOROKNAI, V. et al. Gene Expression Signature of BRAF Inhibitor Resistant Melanoma Spheroids. **Pathology and Oncology Research**, v. 26, n. 4, p. 2557–2566, 1 out. 2020. http://link.springer.com/10.1007/s12253-020-00837-9

LEE, K.-H.; KIM, T.-H. Recent Advances in Multicellular Tumor Spheroid Generation for Drug Screening. **Biosensors**, v. 11, n. 11, p. 445, 11 nov. 2021. https://www.mdpi.com/2079-6374/11/11/445

MAAS-SZABOWSKI, N.; STÄRKER, A.; FUSENIG, N. E. Epidermal tissue regeneration and stromal interaction in HaCaT cells is initiated by TGF- α. **Journal of Cell Science**, v. 116, n. 14, p. 2937–48, 2003. https://journals.biologists.com/jcs/article/116/14/2937/27275/Epidermal-tissue-regeneration-and-stromal

MBEUNKUI, F.; JOHANN, D. J. Cancer and the tumor microenvironment: a review of an essential relationship. **Cancer Chemother Pharmacol**, v. 63, n. 4, p. 571–582, 2009. http://link.springer.com/10.1007/s00280-008-0881-9

MEHTA, G. et al. Opportunities and challenges for use of tumor spheroids as models to test drug delivery and efficacy. **Journal of Controlled Release**, v. 164, n. 2, p. 192–204, 10 dez. 2012. https://linkinghub.elsevier.com/retrieve/pii/S016836591200404X

NATH, S.; DEVI, G. R. Three-Dimensional Culture Systems in Cancer Research: Focus on Tumor Spheroid Model. **Pharmacol Ther.**, v. 163, p. 94–108, 2016. https://doi.org/10.1016/j.pharmthera.2016.03.013

NUNES, A. S. et al. 3D tumor spheroids as in vitro models to mimic in vivo human solid tumors resistance to therapeutic drugs. **Biotechnology and Bioengineering**, v. 116, n. 1, p. 206–226, 1 jan. 2019.. https://onlinelibrary.wiley.com/doi/10.1002/bit.26845

QUE, S. K. T.; ZWALD, F. O.; SCHMULTS, C. D. Cutaneous squamous cell carcinoma. **Journal of the American Academy of Dermatology**, v. 78, n. 2, p. 237–247, 1 fev. 2018. https://linkinghub.elsevier.com/retrieve/pii/S0190962217323253

PARENTE, K. et al. Expressão de AKR1B10 e os efeitos citotóxicos da 22β-hidroxitingenona em carcinoma de células escamosas. **Peer Review**, v. 5, n. 12, p. 320–337, 14 jun. 2023. https://peerw.org/index.php/journals/article/view/517

RAMA-ESENDAGLI, D. et al. Spheroid formation and invasion capacity are differentially influenced by co-cultures of fibroblast and macrophage cells in breast cancer. **Molecular biology reports**, v. 41, n. 5, p. 2885–2892, 2014. https://pubmed.ncbi.nlm.nih.gov/24469725/

REIJNDERS, C. M. A. et al. Development of a Full-Thickness Human Skin Equivalent in Vitro Model Derived from TERT-Immortalized Keratinocytes and Fibroblasts. **Tissue Engineering - Part A**, v. 21, n. 17–18, p. 2448–2459, 2015. https://www.liebertpub.com/doi/10.1089/ten.tea.2015.0139

SAKALEM, M. E. et al. Historical evolution of spheroids and organoids, and possibilities of use in life sciences and medicine. **Biotechnology Journal**, v. 16, n. 5, p. 2000463, 25 maio 2021. https://onlinelibrary.wiley.com/doi/10.1002/biot.202000463

SHIMIZU, I. et al. Treatment of Squamous Cell Carcinoma In Situ : A Review. **Dermatologic Surgery**, v. 37, n. 10, p. 1349–1411, 2011. https://journals.lww.com/00042728-201110000-00002

SONG, A. S.; NAJJAR, A. M.; DILLER, K. R. Thermally induced apoptosis, necrosis, and heat shock protein expression in 3D culture. **Journal of Biomechanical Engineering**, v. 136, n. 7, 2014. https://asmedigitalcollection.asme.org/biomechanical/article/doi/10.1115/1.4027272/472860/Thermally-Induced-Apoptosis-Necrosis-and-Heat

SPOERRI, L.; GUNASINGH, G.; HAASS, N. K. Fluorescence-Based Quantitative and Spatial Analysis of Tumour Spheroids: A Proposed Tool to Predict Patient-Specific Therapy Response. **Frontiers in Digital Health**, v. 3, 28 maio 2021. https://www.frontiersin.org/articles/10.3389/fdgth.2021.668390/full

STENZEL, K. et al. Alkoxyurea-Based Histone Deacetylase Inhibitors Increase Cisplatin Potency in Chemoresistant Cancer Cell Lines. **Journal of Medicinal Chemistry**, v. 60, n. 13, p. 5334–5348, 13 jul. 2017. https://pubs.acs.org/doi/10.1021/acs.jmedchem.6b01538

SUNG, H. et al. Global Cancer Statistics 2020: GLOBOCAN Estimates of Incidence and Mortality Worldwide for 36 Cancers in 185 Countries. **CA: A Cancer Journal for**

Clinicians, v. 71, n. 3, p. 209–249, 4 maio 2021. https://onlinelibrary.wiley.com/doi/10.3322/caac.21660

VERJANS, E. T. et al. Three-dimensional cell culture models for anticancer drug screening: Worth the effort? **Journal of Cellular Physiology**, v. 233, n. 4, p. 2993–3003, 2018. https://onlinelibrary.wiley.com/doi/10.1002/jcp.26052

WHO. **WHO report on cancer: setting priorities, investing wisely and providing care for all**. Available at: <https://www.who.int/publications-detail/who-report-on-cancer-setting-priorities-investing-wisely-and-providing-care-for-all>. Accessed on: 20 jun. 2023.

ZANONI, M. et al. Anticancer drug discovery using multicellular tumor spheroid models. **Expert Opinion on Drug Discovery**, v. 14, n. 3, p. 289–301, 4 mar. 2019. https://www.tandfonline.com/doi/full/10.1080/17460441.2019.1570129

ZANONI, M. et al. Modeling neoplastic disease with spheroids and organoids. **Journal of Hematology & Oncology**, v. 13, n. 1, p. 97, 16 dez. 2020. https://jhoonline.biomedcentral.com/articles/10.1186/s13045-020-00931-0

ZHANG, K. et al. TUG1/miR-133b/CXCR4 axis regulates cisplatin resistance in human tongue squamous cell carcinoma. **Cancer Cell International**, v. 20, n. 1, 6 maio 2020. https://cancerci.biomedcentral.com/articles/10.1186/s12935-020-01224-9